International Conference on Space Optics—ICSO 2012

Ajaccio, Corse

9–12 October 2012

Edited by Bruno Cugny, Errico Armandillo, and Nikos Karafolas

Laser ranging interferometer for GRACE follow-on

Gerhard Heinzel

Benjmin Sheard

Nils Brause

Karsten Danzmann

et al.

International Conference on Space Optics — ICSO 2012, edited by Bruno Cugny, Errico Armandillo, Nikos Karafolas
Proc. of SPIE Vol. 10564, 1056420 · © 2012 ESA and CNES · CCC code: 0277-786X/17/$18 · doi: 10.1117/12.2309099

Laser Ranging Interferometer for GRACE follow-on

Gerhard Heinzel*, Benjmin Sheard*, Nils Brause*, Karsten Danzmann*, Marina Dehne*,
Oliver Gerberding*, Christoph Mahrdt*, Vitali Müller*, Daniel Schütze*, Gunnar Stede*,
William Klipstein†, William Folkner†, Robert Spero†, Kolja Nicklaus‡, Peter Gath§ and Daniel Shaddock¶
*Max-Planck-Institut für Gravitationsphysik (Albert-Einstein-Institut), Callinstrasse 38,
D-30419 Hannover, Germany , **Email:** gerhard.heinzel@aei.mpg.de
†Jet Propulsion Laboratory, California Institute of Technology, 4800 Oak Grove Drive
Pasadena, CA 91109, United States of America
‡STI Immenstaad
§Astrium Immenstaad
¶Department of Quantum Science, The Australian National University
Building 38a, Science Rd, Acton ACT 0200, Australia

***Abstract*—The Gravity Recovery and Climate Experiment (GRACE) has produced a wealth of data on Earth gravity, hydrology, glaciology and climate research. To continue that data after the imminent end of the GRACE mission, a follow-on mission is planned to be launched in 2017, as a joint US-German project with a smaller Australian contribution. The satellites will be essentially rebuilt as they were for GRACE using microwave ranging as the primary instrument for measuring changes of the intersatellite distance. In addition and in contrast to the original GRACE mission, a Laser Ranging Interferometer (LRI, previously also called 'Laser Ranging Instrument') will be included as a technology demonstrator, which will operate together with the microwave ranging and supply a complimentary set of ranging data with lower noise, and new data on the relative alignment between the spacecraft. The LRI aims for a noise level of 80 nm/$\sqrt{\text{Hz}}$ over a distance of up to 270 km and will be the first intersatellite laser ranging interferometer. It shares many technologies with LISA-like gravitational wave observatories. This paper describes the optical architecture including the mechanisms to handle pointing jitter, the main noise sources and their mitigation, and initial laboratory breadboard experiments at AEI Hannover.**

I. Introduction

The Gravity Recovery and Climate Experiment (GRACE) was launched in March 2002 as a joint US-German mission with a design life of 5 years. The mission was subsequently extended until the end of its on-orbit life, which is imminent at the time of writing (2012).

GRACE measures the Earth's gravity field [1], [2] with a spatial resolution of about 200 km and a typical temporal resolution of one month.

The resulting gravity field solutions have produced a wealth of useful information for geophysics, hydrology, glaciology, climate reasearch and other fields.

GRACE consists of two identical satellites in low circular polar orbits. The tiny variations in the intersatellite range (between 170 km and 270 km) are monitored by a two-way microwave K-band ranging (KBR) link [3]. These variations encode fluctuations of the gravity field at the instantaneous orbit, from which the gravity field can be recovered in a complicated process that involves correction for non-gravitational accelerations (measured by on-board accelerometers), removal of aliasing effects due to ocean and solid-earth tides, correction for atmospheric effects, precise orbit determination using GNSS, etc. This paper is, however, only concerned with the generation of an improved set of raw ranging measurements.

The success of GRACE has led to the decision, triggered by high demand from the user community, to launch a **GRACE follow-on** (GFO) mission as soon as possible to minimize the gap in the data stream. That mission will be a rebuild of the original GRACE mission with as few changes as possible, and the same US-German team partnership. The most significant difference is the additional inclusion of an experimental **Laser Ranging Interferometer** (LRI) as a technology demonstrator. That LRI, the subject of this paper, is designed to measure the same range fluctuations as the KBR instrument, but with less noise, and in addition provides precise measurements of the relative pointing of the satellites to each other. As the LRI is an experimental complimentary instrument, it has less stringent lifetime and reliability requirements than the primary KBR instrument. It is hoped, however, that both instruments can be operated in parallel for a large part of the mission life and thus produce better final results by new combinations of their data, mutual calibration and consistency checks etc. If the LRI performs better than the KBR, as hoped, it will probably be used in future GRACE-type missions as primary instrument. In addition, it will be the first space-based laser interferometer to measure distance variations between remote spacecraft, with significant implications for other missions using the same basic measurement such as LISA [4], [5], [6], [7]. GFO is currently planned to be launched in 2017, and the LRI is a joint US-German development with additional contributions from Australia. A detailed description of the LRI design has recently been published [8], and this paper summarizes the main features with particular emphasis on optics.

II. Laser ranging interferometer architecture

The straightforward approach of routing the laser beam back and forth along the connecting line between the two spacecraft's centers of mass is not possible in GFO since that

path is blocked by existing components such as the KBR horn antennae. Hence an alternative design is used, the so-called 'racetrack' configuration shown in figure 1.

The key geometric element of this design is the system of three mirrors on each spacecraft used to route the beam through each spacecraft. These three mirrors form a corner cube configuration, i.e. their mirror planes are perpendicular to each other. For small rotations of the device the beam spots are nearly stationary and the corner cube doesn't need to be complete — only the actually reflecting segments need to be present. This arrangement has a number of useful special properties: The intersection point of the three mirror planes (the vertex of the retro-reflector) can be located outside the mirror device, allowing the effective fiducial measurement point to be placed inside the accelerometer housing. Additionally two important parameters are invariant under rotation around the vertex, namely:

- the round-trip pathlength, which is twice the distance between the beam starting point and a plane normal to the beam direction and intersecting the vertex,
- the propagation direction of the reflected beam which is always anti-parallel to the incident beam.

These are essential elements to construct a system with high immunity to spacecraft attitude jitter.

The second fundamental ingredient is the frequency domain scheme of offset phase locking. The laser in one of the spacecraft (called S/C 1) in the otherwise perfectly symmetrical setup is designated as master laser and locked in frequency to an on-board reference cavity, to minimize noise originating from laser frequency fluctuations. When arriving at the other spacecraft (S/C 2), the light has picked up a Doppler shift of a few MHz, either positive or negative. Due to the beam divergence and the small apertures necessary to cope with misalignments, less than 1 nW out of 25 mW laser power are received at S/C 2, such that direct retro-reflection is infeasible. Instead, a local laser is phase-locked to the incoming light with a frequency offset chosen such that after picking up once more the Doppler shift (with the same sign) on the way back to S/C 1, the beatnote between the light arriving back at S/C 1 and the local, stabilized, laser at S/C 1 is in the sensitive frequency range of the phasemeter (approximately 2…15 MHz).

Referring to Figure 2, the effective measured lengths can be determined to be

$$s_2 - s_1 = x_1 + y_1 + x_2 + y_2, \tag{1}$$

where s_1 and s_2 are the phasemeter outputs scaled as lengths. Together with the properties of the triple mirror this yields the desired range measurement

$$\frac{s_2 - s_1}{2} = d_1 + d_2. \tag{2}$$

The lenghts $a_{1/2}$ and $b_{1/2}$ cancel to first order, which includes longitudinal errors of the steering mirrors. As a consequence, these pathlengths on the optical bench do not need to be ultra-stable.

III. Top-level requirements

Fig. 3 shows the currently used top-level requirement for the one-way ranging displacement noise as amplitude spectral density.

The most interesting frequency range is between 2 and 100 mHz, which corresponds to spherical harmonics of order 10 to 500 very roughly.

The noise budget for the laser interferometer was chosen according to the following criteria:

- The noise budget discussed here is meant to include all noise sources of the interferometric range measurement, in particular laser frequency noise, pointing-induced noise, stray light, electronic noise etc. It does *not* include noise sources in the downstream data analysis like tide aliasing etc.
- It should be considerably below the present GRACE ranging performance, ideally below other noise sources in the total data processing chain (tide aliasing etc.) such that the interferometer is not limiting the overall performance at any frequency.
- For the same reason it should be lower than the accelerometer noise at low frequencies.
- It cannot be lower than the predicted laser frequency noise contribution.

This results in the following preliminary noise budget for the single-link interferometer ranging noise:

$$\boxed{\tilde{x}(f) < \frac{80\,\mathrm{nm}}{\sqrt{\mathrm{Hz}}} \times \mathrm{NSF}(f) \quad 2\,\mathrm{mHz} < f < 100\,\mathrm{mHz}} \tag{3}$$

which uses the noise-shape function ("NSF")

$$\boxed{\mathrm{NSF}(f) = \sqrt{1 + \left(\frac{f}{3\,\mathrm{mHz}}\right)^{-2}} \times \sqrt{1 + \left(\frac{f}{10\,\mathrm{mHz}}\right)^{-2}}} \tag{4}$$

The overall performance at low frequencies will be limited by the accelerometer performance and the main improvement enabled by the laser ranging interferometer is in the $10\,\mathrm{mHz}$ to $100\,\mathrm{mHz}$ frequency band, corresponding to spatial scales of $770\,\mathrm{km}$ to $77\,\mathrm{km}$ for an orbital velocity of $\approx 7.7\,\mathrm{km/s}$.

IV. Noise sources

In the LRI the two dominant noise sources expected are laser frequency noise and pointing induced noise. The equivalent coupling factor for laser frequency noise can be expressed as

$$\widetilde{\delta x} = \frac{\rho}{\nu}\,\widetilde{\delta\nu} \tag{5}$$

where $\widetilde{\delta\nu}$ is the linear spectral density of the laser frequency noise, ν is the laser frequency, ρ the satellite separation, assumed to be $< 270\,\mathrm{km}$ and $\widetilde{\delta x}$ is the resulting ranging noise.

Approximately half of the total single-link noise budget has been allocated to laser frequency noise, and the resulting required stability level of about $30\,\mathrm{Hz}/\sqrt{\mathrm{Hz}}$ will be achieved by

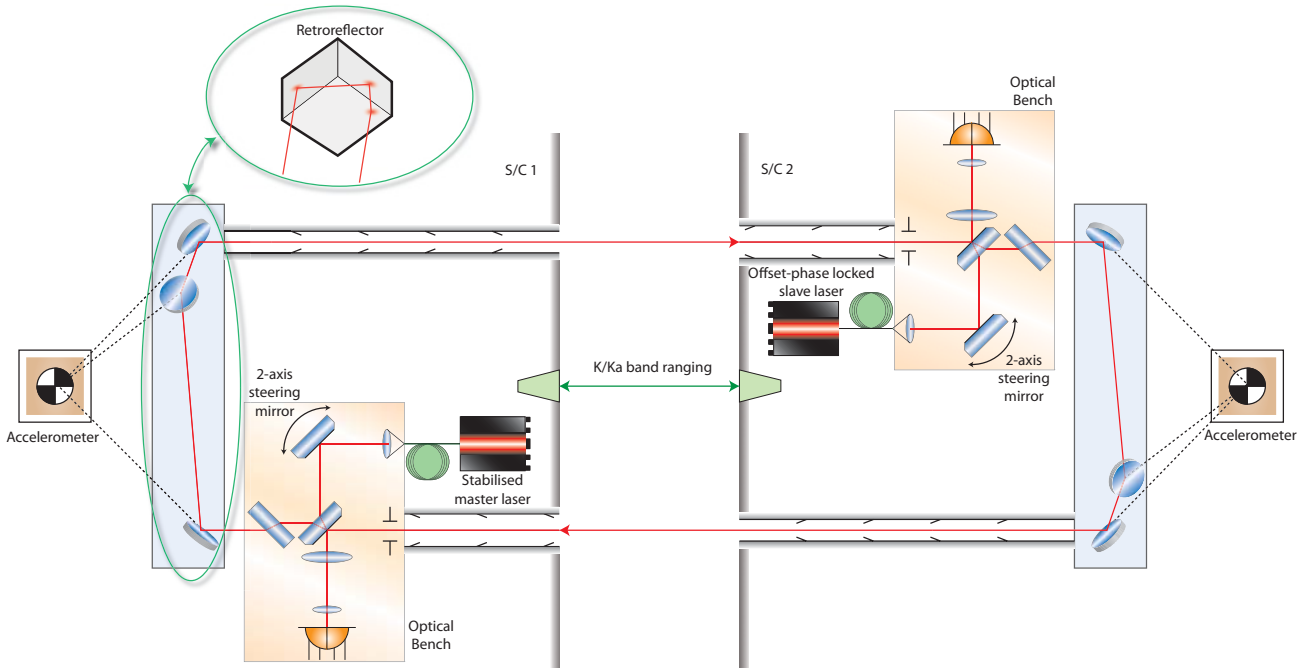

Fig. 1. Optical layout for the laser ranging interferometer (Laser frequency stabilisation subsystem not shown). The microwave ranging system is labelled K/Ka band ranging is centered on axis. Figure taken from [8].

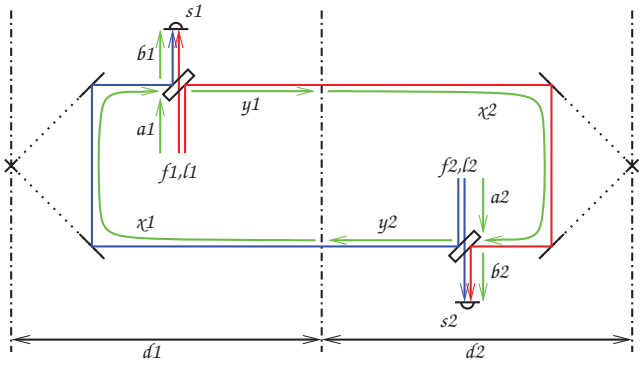

Fig. 2. Sketch of the measured lengths. Red lines indicate the higher laser frequency f_1, blue lines the lower laser frequency f_2 and green arrows distances, measured to the interfering surface of the beamsplitter.$l_{1/2}$ represent the laser phase fluctuations expressed as equivalent lengths. A reference plane between the spacecraft has been added for convenience of notation, it has no physical meaning.

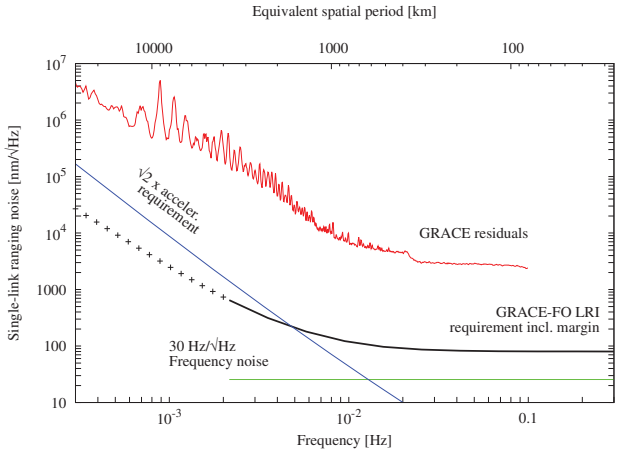

Fig. 3. Top-level requirement for the one-way ranging displacement noise. For comparison the topmost curve shows one example of post-fit residuals of the GRACE microwave ranging data, which represent an upper limit of the noise of that instrument. The frequency noise is scaled for an assumed range of 240 km.

locking the master laser to a reference cavity using the Pound-Drever-Hall scheme [9], [10], [11], [12]. Both satellites will carry identical hardware, in particular including a reference cavity. Only one of them is required and will be active at any time, thus providing for limited redundancy.

Pointing induced noise can be caused by offsets of the retro-reflector vertex from the accelerometer reference point, phase changes due to beam walk effects and far-field curvature errors. They are typically the product of a static imperfection such as the vertex offset (e.g. 50 μm) and the spacecraft pointing fluctuations (e.g. 0.5 mrad/$\sqrt{\text{Hz}}$). The latter are determined by the AOCS system of the spacecraft and cannot be influenced by the LRI, furthermore their range and spectrum are not well known at this time. Hence mitigating the pointing induced noise can only be achieved by minimizing the static imperfections, using sufficient margins and conservative assumptions for the spacecraft AOCS behaviour.

Optical pathlength variations unrelated to gravitational forces, for example due to thermal effects, also lead to measurement errors. The thermal variations are expected to

have significant quasi-periodic variations corresponding to the orbit frequency and its harmonics. Hence the temperature-dependent dimensional stability of components in the sensitive optical path is most critical. An advantage of the proposed design is that the main sensitive path contains only a few simple components, while the dimensional stability of the other components couples only via second order effects. This relaxes in particular the length stability requirements for the steering mirror and imaging optics.

Readout noise is predicted to be well below the other noise sources and includes:

- USO noise
- Shot noise
- Laser power noise
- Photodetector electronic noise
- Parasitic signals (e.g. scattered light and electronic cross-talk)
- ADC quantization noise
- Spurious electronic phaseshifts

While clearly these noise sources must and will be estimated and budgeted in detail, they also occur in similar form in LISA with its 1000 times more stringent pathlength noise requirements, where they have been studied in detail and found to be manageable by proper design choices.

V. Optical bench

Fig. 4 shows a schematic of the present optical bench design, which will be rigidly mounted to the main equipment platform of the spacecraft. The light from the laser (a few 10 mW at 1064 nm) is delivered to the optical bench by a single-mode polarization-maintaining optical fiber, after a small fraction has been split off for the frequency stabilisation subsystem (active in one S/C only). The fiber injector collimates and shapes the beam coming out of the fiber such that a nearly Gaussian beam waist of 2.5 mm radius is located on the 2-D steering mirror. The beam is then directed to the beamsplitter which has a high reflectivity, e.g. 95 %, such that most of the light is directed towards the distant spacecraft and the remaining few percent are transmitted and pass through a lens system to the quadrant photodetector where they act as local oscillator (reference beam).

The first function of the lens system is to simultaneously image both the receive aperture and the steering mirror pivot plane onto the photodetector such that a beam tilt at either the aperture or steering mirror leads to a pure tilt (i.e. without beam walk) on the photodetector (see Section VII). To achieve the correct imaging for both beams, the steering mirror and the aperture on the optical bench must have the same effective distance from the lens system. In addition the imaging system is used to match the beam size to the (smaller) quadrant photodetector.

A high-fidelity optical imaging in the classical sense is not necessary here, since the quadrant photodetector has only four 'pixels'. The main requirement is a small coupling of tilt into the length measurement. Aberrations of the imaging system are largely common to both beams. The remaining residual

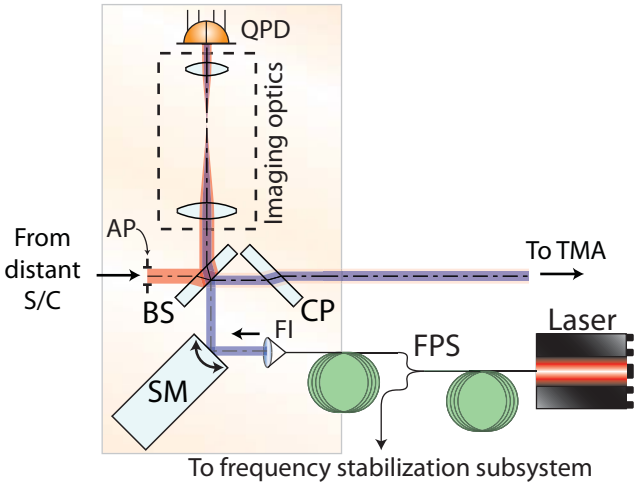

Fig. 4. Optical bench layout. The local beam waist is located on the steering mirror. AP - aperture, BS - beamsplitter, CP - compensation plate, FI - fiber injector, FPS - fiber power splitter, QPD - quadrant photodetector, SM - steering mirror. Figure taken from [8].

coupling is mainly caused by the different spatial profile of the two beams and residual beam misalignments.

The pathlength through a single beamsplitter is angle dependent which leads to a coupling of the spacecraft attitude jitter into the round-trip length measurement. The coupling factor for yaw is dominant and amounts to 2.2 mm/rad for a 7 mm thick fused silica beamsplitter. For pitch the coupling factor is quadratic and nominally at a turning point. These coupling factors as a function of spacecraft rotation are shown in Fig. 5 .

The yaw coupling factor of 2.2 mm/rad is too large by about 20 . . . 50 times for typical assumed spacecraft pointing jitter and noise budgets. It can be almost completely removed by adding a compensation plate made from the same material as the main beamsplitter but rotated by 90 degrees. This shifts the coupling factor for yaw also to a nominal minimum working point. The coupling factor with a 1 mrad error from the nominmal minimum amounts to only 10 μm/rad with the compensation plate. These coupling factors were estimated using simple raytracing along the sensitive path of the interferometer and for nominally perfect geometry. A detailed analysis of the optical bench and its pathlength performance is given in [13].

VI. Satellite pointing

The orientation of the GRACE satellites to each other is controlled to a level of a few mrad based on the orbits of the satellites and star cameras. Actuators are magnetic torque rods and cold gas thrusters in case the Earth's magnetic field lines are unfavourably aligned or if the disturbances are such that the magnetic torque rods have insufficient control authority [14]. GRACE-FO will use the same basic attitude control scheme. While this level of attitude control is sufficient for the microwave ranging system due its wide beam and receive field of view, these misalignments are too large for the

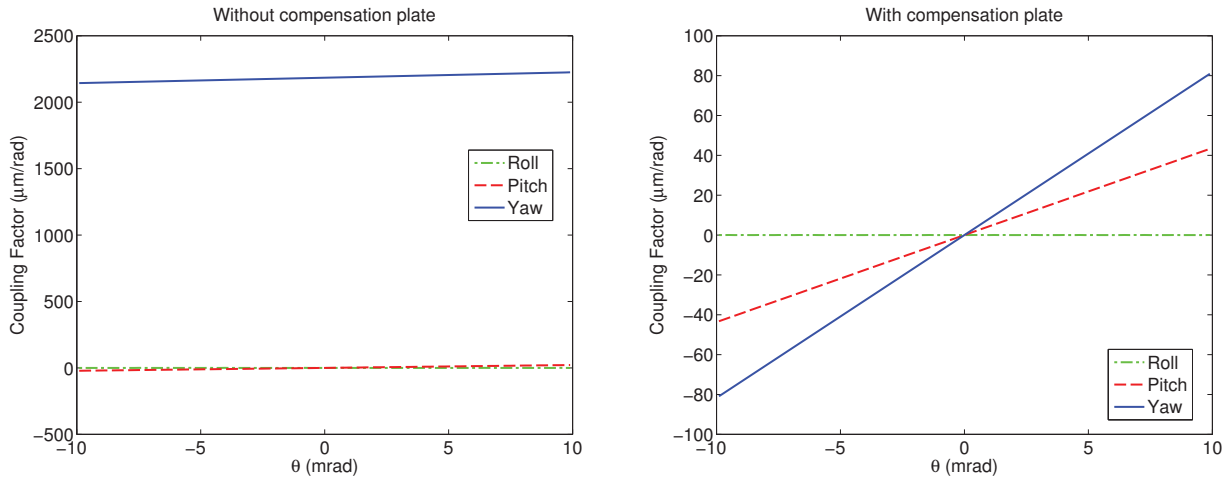

Fig. 5. Coupling factors for pitch, yaw and roll into the sensitive pathlength for only the beamsplitter (shown on the left) and for both the beamsplitter and compensation plate (shown on the right). Figure taken from [8].

laser interferometer, which requires about 100 μrad pointing accuracy. Therefore active pointing control is required.

In future missions the required pointing accuracy could be potentially achieved by improved spacecraft pointing control, ideally based on optical measurements from the laser interferometer itself. For the GFO LRI instrument discussed here, the pointing control must, however, be implemented internally in the instrument itself. The Differential Wavefront Sensing function of the interferometer is used as sensor, and a single steering mirror per spacecraft as actuator that simultaneously optimizes the interferometer contrast in the receive path as well as the transmit beam pointing. These functions are discussed in the following sections.

Beam pointing control does not eliminate the coupling of spacecraft jitter completely from the measurement, since the spacecraft still has a variable physical misalignment which leads to varying beam paths. For example an offset of the triple mirror vertex from the accelerometer reference point (the effective rotation point after using the accelerometer output in data processing) leads to a coupling of satellite attitude jitter into the measured round-trip length variations. Typical numbers lead to a static alignment requirement of the order of 100 μm for the vertex location in the two directions orthogonal to the beam axis. Other effects that also lead to such coupling include effects on the optical bench such as incomplete compensation of the beamsplitter pathlength error by the compensation plate, differential-mode aberrations in the beam compressor lens system, stray light and diffraction effects in the triple mirrors and baffles, etc. It is expected that these effects will be mostly a systematical and reproducible function of the 2-D pointing error of the spacecraft, such that they can be at least partially removed in data postprocessing if an accurate measurement of the instantaneous pointing error is available. In the LRI, the feedback signal fed to the steering mirror will serve this purpose and will therefore be recorded and downloaded as science data.

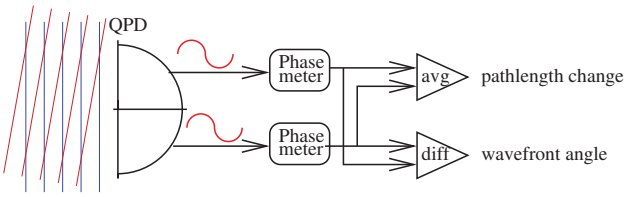

Fig. 6. Differential wavefront sensing principle.

VII. Differential Wavefront Sensing and Steering Mirror Control

Differential wavefront sensing (DWS) is a well known technique for measuring with high sensitivity the angle between two wavefronts in a laser interferometer (see for example [15], [16], [17], [18], [19]). Fig. 6 illustrates the basic principle of DWS.

The photodetector is split into 4 segments which are connected to separate phasemeter channels. The average of the measured phases represents the pathlength signal similar to what a single-element diode would produce, and the difference between 'left' and 'right' or 'top' and 'bottom' represents the angle between the wavefronts in horizontal and vertical direction, respectively.

The conversion factor from geometrical angle to electrical phase difference can be very large and contributes to the high sensitivity of the method. With some simplifying assumptions it is given by

$$k \approx \frac{16r}{3\lambda} \tag{6}$$

for the case two flat-top beams, where r is the beam radius and λ is the optical wavelength.

Numerical simulations using the methods described in [20] yield factors of about 20000 rad/rad for the real situation of one Gaussian and one flat-top beam and the planned LRI parameters.

Further benefits of the DWS sensing method are that the result is to first order independent of small lateral movements of the photodiode (or, equivalently, a common-mode beam walk of both beams), and that many noise sources of the pathlength measurement such as laser frequency noise cancel. In laboratory experiments with comparable parameters, sensitivities of a few nrad/$\sqrt{\text{Hz}}$ have been reached (see, e.g., [21]).

In future missions it may be optimal to use that DWS signal to directly control the spacecraft attitude, since a 'zero' DWS signal also corresponds to optimal contrast and lowest noise in the interferometric length measurement. This is, however, not possible for the GFO LRI discussed here for programmatic reasons (no major change w.r.t. GRACE allowed, reduced reliability requirements for LRI). Hence the DWS signal must be used differently to ensure optimal LRI operation in the presence of large spacecraft jitter. One option would have been to move the entire optical bench, which has the advantage that the optical path is stationary within the optical bench. This has, however, been discarded in favour of the steering mirror described below, since the bench is heavy, its motion thus slow and incompatible with fast scanning for acquisition, and might furthermore disturbe the nearby accelerometer.

In the LRI case the DWS signal represents the relative angle between the received beam and the local oscillator beam. Since the optical bench is rigidly mounted in the spacecraft, the angle of the received beam w.r.t. the optical bench represents the misalignment of the local spacecraft's optical axis w.r.t. to the the other spacecraft. The angle of the local oscillator beam w.r.t. the optical bench, on the other hand, is directly controlled by and only depends on the steering mirror.

Fig. 7 illustrates the principle of operation of the steering mirror control loop.

Three situations are shown. The first is the nominal situation where the incoming beam and the local beam are aligned. The illustration in the middle shows the situation when the spacecraft alignment changes, leading to a non-zero DWS signal and also to a misalignment between the incoming and outgoing beam directions. Consequently, both the local heterodyne efficiency and the power received at the other specacraft decrease. Closing the steering mirror control loop (right part of Fig. 7) zeros the DWS signal by rotating the steering mirror until the local and incoming beams are parallel on the photodetector. This yields not only optimal interference contrast on the photodetector, but also ensures that local and received beam are parallel at the beamsplitter BS. Together with the second property of the triple mirror listed in Section II, this leads to the outgoing beam being parallel to the incoming beam, independent of the local spacecraft orientation. The transmitted beam thus always points back to the other spacecraft, and the local spacecraft can be considered an "active retroreflector". This very useful behaviour only occurs when no lenses or other curved optical elements are included in the main round-trip beam path, since such elements would change the beam direction. As a consequence, the same unmodified laser beam needs to serve both as transmit beam on the long arm and as local oscillator for the receive beam. A detailed investigation of possible beam parameters resulted in the choices listed in Table I.

Parameter	Value	Units
Receive aperture radius	4	mm
Transmit beam waist radius	2.5	mm
Laser power	25	mW
Laser wavelength	1064	nm
Satellite separation	270	km
Transmission efficiency for receive path	97	%
Transmit efficiency	50	%
Effective received power (a)	≈ 200	pW
Effective received power (b)	> 25	pW

TABLE I
Parameters chosen as baseline design. The value for the "Transmission efficiency for receive path" parameter includes the reflection from the beamsplitter and loss in the imaging optics, but neither the photoreciever efficiency nor the heterodyne efficiency. The heterodyne efficiency is however included in the effective power computation. The "Transmit efficiency" includes the fiber power splitter, transmission through the components on the optical bench and the TMA. Case (a) for the effective received power applies to perfect alignment, while case (b) represents a misalignment of both transmitter and receiver of 100 μrad each. This misalignment is not the actual spacecraft orientation, but only the beam pointing error due to residual errors and offsets in the beam steering control loop and optics.

As described in Section VI, information about the real spacecraft pointing is still required to compensate residual coupling effects of that pointing into the pathlength measurement. As the DWS signal has been driven to near zero by the loop, it is not useful for that purpose any more, but the information must be obtained from the feedback signal to the steering mirror instead. This requires either a very linear and predictable mirror actuator, or an internal sensor within the actuator that yields an accurate representation of the actual mirror angle.

VIII. Breadboard experiments

Laboratory experiments are ongoing at AEI Hannover to verify the basic functionality and critical performance parameters of the instrument using breadboard models of the components. It is planned to use similar test setups later for the industrial engineering and flight models. Apart from the basic function, i.e. the capability to measure the roundtrip pathlength, the most important properties to be tested have to do with the behaviour under rotation. Therefore a commercial Hexapod (PI model M824.VG) is used as platform for the optical elements under test and is programmed to rotate about variable pivot points.

The readout is performed using a heterodyne laser interferometer operating at 1064 nm and a heterodyne frequency of a few MHz (6 MHz at the moment), which is achieved by phase-locking the second laser with that offset using a fixed reference interferometer. A phasemeter breadboard developed in the context of LISA is used to record the phase of the beatnotes.

The first experiment aimed at finding the vertex of a given triple mirror and is sketched in Figure 8.

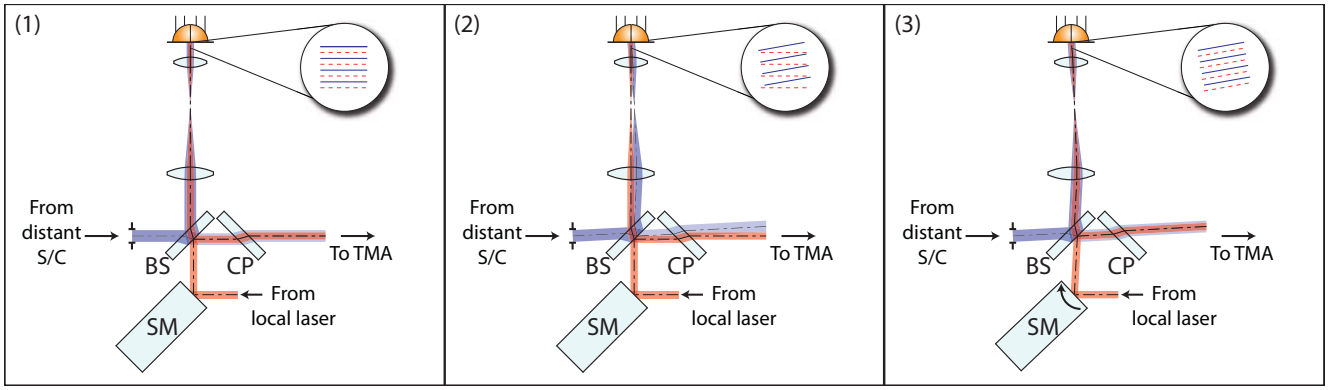

Fig. 7. Function of the steering mirror control loop. From left to right: (1) nominal situation with spacecraft perfectly aligned, (2) spacecraft misalignment produces a non-zero DWS signal on the photodetector, (3) feedback to steering mirror makes DWS signal zero and makes outgoing beam parallel to incoming beam. SM - steering mirror, BS - beamsplitter, CP - compensation plate. Figure taken from [8].

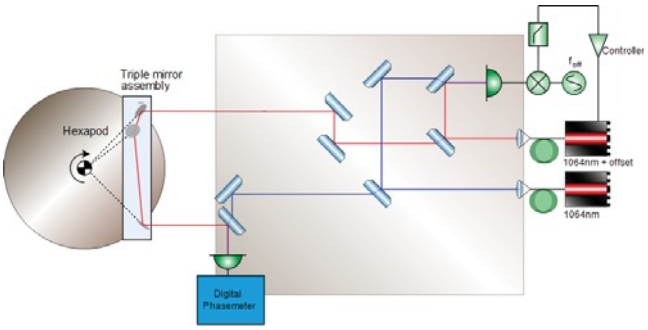

Fig. 8. Laboratory test setup to determine the vertex of a triple mirror.

The triple mirror under test is mounted onto the Hexapod and rotated about 3 axes around a fixed pivot point. The pathlength changes during the rotation are recorded with the phasemeter. If the hexapod pivot coincides with the triple mirror vertex, the pathlength change as a function of rotation angle is small and has in general a quadratic dependency. Otherwise, the pathlength has a large linear dependence on the rotation angle. This measurement is repeated for a grid of hexapod rotation points. By least-squares fitting the data to a model based on optical raytracing, the 'point of minimal coupling' (PMC) of the triple mirror can be found with an accuracy of roughly $50 \ldots 100\,\mu$m in the two transversal directions. The third direction (along the beam) is much less sensitive. The PMC thus determined coincides with the vertex of the triple mirror only if the mirror planes intersect at exact right angles. Otherwise, only the PMC can be found with this method, which is, however, also the relevant point for instrument integration. The accuracy of the result is limited by the repeatability and accuracy of the hexapod motion. Therefore an auxiliary 6-degree-of-freedom interferometer is under development which will monitor the actual hexapod motion with higher interferometric accuracy.

The second experiment, shown in Figure 9, tests the functions of the optical bench including its transponder function, beam compressor imaging system and steering mirror, and the steering mirror control loop.

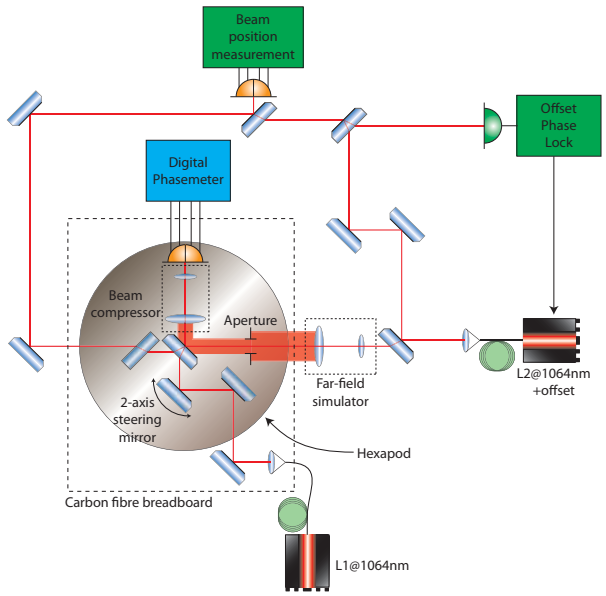

Fig. 9. Laboratory test setup to test a breadboard of the optical bench.

A beam expander produces a spatially fixed beam wide enough such that the receive aperture cuts out a flat-top beam. The optical bench works as described in the previous sections. A picture of the breadboard optical bench used in this experiment is shown in Figure 10.

The measurement consists in comparing the two phasemeter readings, one of which is again driven to near zero by the offset phase lock that controls the frequency of the second laser. The optical bench is used in transmission, and the properties to be verified under rotation and translation of the optical bench are:

- Invariance of the direction of the outgoing beam,
- Maintaining high contrast and DWS $= 0$,
- Invariance of round-trip pathlength.

All of these have been verified experimentally, and detailed results will be the subject of another publication.

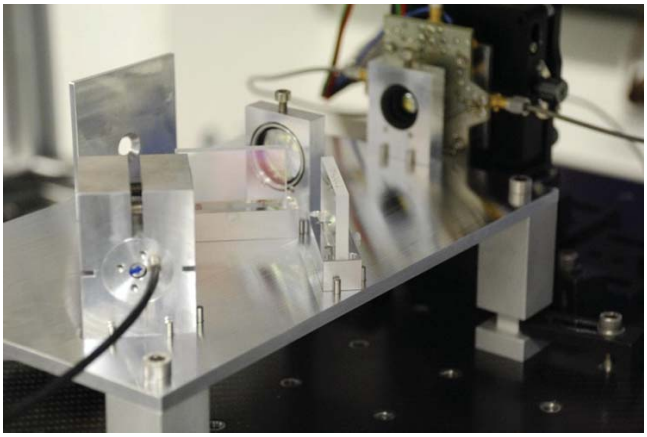

Fig. 10. Breadboard of the optical bench.

The next measurement being planned at the moment is shown in Figure 11 and combines both triple mirror and optical bench on one platform (a carbon-fibre breadboard) that is rotated by the Hexapod.

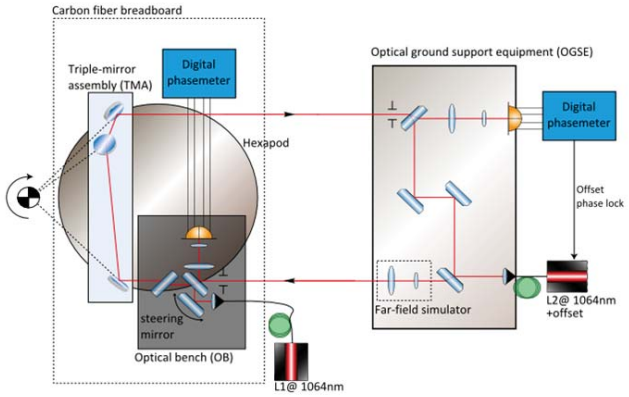

Fig. 11. Planned test setup to for both TMA and optical bench.

Other simulations and experiments taking place at AEI Hannover, ANU Canberra, Astrium and JPL study the nontrivial problem of initial lock acquisition. The phasemeters can only measure a signal if 5 degrees of freedom are all within small limits simultaneously: 2 angles at the transmitter and receiver each, and the laser frequency difference. Therefore all these 5 degrees of freedom must be scanned according to some predetermined pattern. Complications arise since there is no direct communication between the satellites, and it is not guaranteed that a signal of marginal strength is simultaneously detected at both ends. We now believe that a relatively straightforward, robust algorithm will work, which will be described in a separate publication. Both the average and the worst-case time depend critically on the expected absolute error of the initial alignment estimate and on the maximal scan speed of the steering mirror. These two quantities are therefore of critical importance for the robust function of the whole LRI.

IX. Conclusion

The Laser Ranging Interferometer (LRI) for Grace Follow-On (GFO) employs a novel optical architecture that allows precision interspacecraft ranging in the presence of large misalignments. First breadboard experiments verify analytical and numerical predictions. The LRI will be launched in 2017 and will be the first intersatellite laser interferometer. Apart from its immediate use to provide improved ranging data for the GFO mission, it will serve as technology demonstrator for future GRACE-type missions as well as for gravitational wave observatories like LISA.

Acknowledgment

This work was partly funded by the "Deutsche Forschungsgemeinschaft" (DFG) within the Cluster of Excellence QUEST (Centre for Quantum Engineering and Space-Time Research). Parts of the research described in this publication were carried out at the Jet Propulsion Laboratory, California Institute of Technology, under a contract with the National Aeronautics and Space Administration. This work was also supported under the Australian Government's Australian Space Research Program.

References

[1] Tapley BD, Chambers DP, Bettadpur S, Ries JC (2003) *Large scale ocean circulation from the GRACE GGM01 Geoid.* Geophys Res Lett 30(22):2613

[2] Tapley BD, Bettadpur S, Watkins M, Reigber C (2004b) *The Gravity Recovery and Climate Experiment: Mission Overview and Early Results.* Geophys Res Lett 31(9):L09,607

[3] Dunn C, Bertiger W, Bar-Sever Y, Desai S, Haines B, Kuang D, Franklin G, Harris I, Kruizinga G, Meehan T, Nandi S, Nguyen D, Rogstad T, Thomas JB, Tien J, Romans L, Watkins M, Wu SC, Bettadpur S, Kim J (2003) *Instrument of Grace: GPS Augments Gravity Measurements.* GPS World 14:16–28

[4] Danzmann K, the LISA Science Team (2003) *LISA – An ESA cornerstone mission for the detection and observation of gravitational waves.* Adv Space Res 32(7):1233–1242

[5] Danzmann K, Rüdiger A (2003) *LISA technology–concept, status, prospects.* Class Quantum Gravity 20:S1

[6] Heinzel G, Braxmaier C, Danzmann K, Gath P, Hough J, Jennrich O, Johann U, Rüdiger A, Sallusti M, Schulte H (2006) *LISA interferometry: recent developments.* Class Quantum Gravity 23:S119

[7] Shaddock DA (2008) *Space-based gravitational wave detection with LISA.* Class Quantum Gravity 25:114,012

[8] B. S. Sheard, G. Heinzel, K. Danzmann, D. A. Shaddock, W. M. Klipstein, W. M. Folkner: *Intersatellite laser ranging instrument for the GRACE follow-on mission*, Journal of Geodesy 2012, DOI: 10.1007/s00190-012-0566-3

[9] Drever RWP, Hall JL, Kowalski FV, Hough J, Ford GM, Munley AJ, Ward H (1983) *Laser Phase and Frequency Stabilization Using an Optical Resonator.* Appl Phys B 31(2):97–105

[10] Black ED (2001) *An introduction to Pound–Drever–Hall laser frequency stabilization.* Am J Phys 69(1):79–87

[11] Folkner WM, de Vine G, Klipstein WM, McKenzie K, Shaddock D, Spero R, Thompson R, Wuchenich D, Yu N, Stephens M, Leitch J, Davis M, de Cino J, Pace C, Pierce R (2010) *Laser Frequency Stabilization for GRACE-II.* In: Proceedings of the 2010 Earth Science Technology Forum

[12] Folkner WM, de Vine G, Klipstein WM, McKenzie K, Spero R, Thompson R, Yu N, Stephens M, Leitch J, Pierce R, Lam TTY, Shaddock DA (2011) *Laser Frequency Stabilization for GRACE-2.* In: Proceedings of the 2011 Earth Science Technology Forum

[13] Vitali Müller, M.Sc. thesis, Leibniz University Hannover, October 2012.

[14] Herman J, Presti D, Codazzi A, Belle C (2004) *Attitude Control for GRACE: The first low-flying satellite formation.* In: Proceedings of the 18th International Symposium on Space Flight Dynamics

[15] Morrison E, Meers BJ, Robertson DI, Ward H (1994a) *Experimental demonstration of an automatic alignment system for optical interferometers.* Appl Opt 33(22):5037–5040

[16] Morrison E, Meers BJ, Robertson DI, Ward H (1994b) *Automatic alignment of optical interferometers.* Appl Opt 33(22):5041–5049

[17] Heinzel G, Rüdiger A, Schilling R, Strain K, Winkler W, Mizuno J, Danzmann K (1999) *Automatic beam alignment in the Garching 30-m prototype of a laser-interferometric gravitational wave detector.* Opt Commun 160:321–334

[18] Heinzel G, Rüdiger A, Schilling R, Strain K, Winkler W, Mizuno J, Danzmann K (1999) *Corrigendum to "Automatic beam alignment in the Garching 30-m prototype of a laser-interferometric gravitational wave detector" [Opt. Commun. 160 (1999) 321–334].* Opt Commun 164:161

[19] Heinzel G, Wand V, García A, Jennrich O, Braxmaier C, Robertson D, Middleton K, Hoyland D, Rüdiger A, Schilling R, Johann U, Danzmann K (2004) *The LTP interferometer and phasemeter.* Class Quantum Gravity 21:S581–S587

[20] Wanner, G. et al: *Methods for simulating the readout of lengths and angles in laser interferometers with Gaussian beams*, Optics communications, 2012. doi:10.1016/j.optcom.2012.07.123

[21] Heinzel, G. et al: *Successful testing of the LISA Technology Package (LTP) interferometer engineering model*, Class. Quantum Grav. 22 (2005) 149–154, doi:10.1088/0264-9381/22/10/003